Journal of Pathology
J Pathol 2016; **238:** 63–73
Published online 19 October 2015 in Wiley Online Library (wileyonlinelibrary.com) DOI: 10.1002/path.4636

ORIGINAL PAPER

The genomic landscape of epithelioid sarcoma cell lines and tumours

Farzad Jamshidi,[1] Ali Bashashati,[2] Karey Shumansky,[2] Brendan Dickson,[3,4] Nalan Gokgoz,[4] Jay S Wunder,[5] Irene L Andrulis,[4,6] Alexander J Lazar,[7] Sohrab P Shah,[2,8,9] David G Huntsman[1,8] and Torsten O Nielsen[1,8]*

[1] *Genetic Pathology Evaluation Centre, Vancouver, BC, Canada*
[2] *BC Cancer Research Centre, Vancouver, BC, Canada*
[3] *Department of Pathology and Laboratory Medicine, Mount Sinai Hospital, University of Toronto, Toronto, ON, Canada*
[4] *Lunenfeld-Tanenbaum Research Institute, Mount Sinai Hospital, Toronto, ON, Canada*
[5] *Division of Orthopaedic Surgery, University of Toronto, ON, Canada*
[6] *Departments of Molecular Genetics and Laboratory Medicine and Pathobiology, University of Toronto, ON, Canada*
[7] *The University of Texas MD Anderson Cancer Center, Houston, TX, USA*
[8] *Department of Pathology and Laboratory Medicine, University of British Columbia, Vancouver, BC, Canada*
[9] *Department of Molecular Oncology, BC Cancer Agency, Vancouver, BC, Canada*

**Correspondence to: TO Nielsen, Anatomical Pathology, JPN 1401, Vancouver Hospital & Health Sciences Centre, 855 W 12th Avenue, Vancouver, BC, Canada, V5Z 1M9. E-mail: torsten@mail.ubc.ca*

Abstract

We carried out whole genome and transcriptome sequencing on four tumour/normal pairs of epithelioid sarcoma. These index cases were supplemented with whole transcriptome sequencing of three additional tumours and three cell lines. Unlike rhabdoid tumour (the other major group of SMARCB1-negative cancers), epithelioid sarcoma shows a complex genome with a higher mutational rate, comparable to that of ovarian carcinoma. Despite this mutational burden, *SMARCB1* mutations remain the most frequently recurring event and are probably critical drivers of tumour formation. Several cases show heterozygous *SMARCB1* mutations without inactivation of the second allele, and we explore this further *in vitro*. Finding *CDKN2A* deletions in our discovery cohort, we evaluated CDKN2A protein expression in a tissue microarray. Six out of 16 cases had lost CDKN2A in greater than or equal to 90% of cells, while the remaining cases had retained the protein. Expression analysis of epithelioid sarcoma cell lines by transcriptome sequencing shows a unique profile that does not cluster with any particular tissue type or with other SWI/SNF-aberrant lines. Evaluation of the levels of members of the SWI/SNF complex other than SMARCB1 revealed that these proteins are expressed as part of a residual complex, similarly to previously studied rhabdoid tumour lines. This residual SWI/SNF is susceptible to synthetic lethality and may therefore indicate a therapeutic opportunity.

Keywords: epithelioid sarcoma; next-generation sequencing; *SMARCB1*; genomic landscape

Received 30 June 2015; Revised 22 August 2015; Accepted 7 September 2015

No conflicts of interest were declared

Introduction

Originally described as a variant of synovial sarcoma [1,2] and as *sarcoma aponeuroticum* [3], epithelioid sarcoma was established as a unique entity by Franz M Enzinger in 1970 [4]. Epithelioid sarcoma typically occurs in the distal extremities of young adults, has a predilection towards men [4], and is one of the commonest soft tissue sarcomas of the hand [5]. This form of cancer has a deceptively benign presentation and slow growth at the primary site; however, it is aggressive, with very high recurrence and metastatic rates and hence a very poor long-term survival [5]. Histology shows enlarged atypical cells with prominent nucleoli but otherwise open chromatin; an interesting feature is the formation of pseudogranulomas consisting of tumour cells surrounding a central necrotic area [4]. In 1997, a 'proximal-type' variant of epithelioid sarcoma was described, with large-cell cytomorphology, rhabdoid features, and an increased cellular atypia [6]. Tumours with this histology tended to occur more proximally, for example in the pelvis, perineum, and proximal extremities [6]; nevertheless, the 'classic' versus 'proximal' classification represents a histological, rather than anatomical, distinction.

Immunoreactivity for mesenchymal markers such as vimentin and epithelial markers such as pan-cytokeratin are defining features of epithelioid sarcoma [5], reflecting its combined mesenchymal and epithelial phenotype. Another key immunohistochemical feature is loss of SMARCB1, a core member of the SWI/SNF chromatin-remodelling complex (Supplementary

Figure 1). Fluorescent *in situ* hybridization (FISH) analyses of the breakpoints of rare cases with translocations identified the inactivation of *SMARCB1* as a common event in epithelioid sarcoma [7]. Later, SMARCB1 protein was shown to be lost in the vast majority of cases using immunohistochemistry [8]. However, whether this is due to genetic or epigenetic events has been a subject of much recent debate. Some groups have suggested that most cases lack *SMARCB1* mutations [9,10], while others have stated the opposite [11–13]. Two studies have suggested microRNA species as candidates that could explain loss of SMARCB1 protein [14,15] in the presence of intact alleles.

In addition to epithelioid sarcoma, an increasing number of tumours have been recognized to lack SMARCB1 expression [16]. Among these, extra-renal malignant rhabdoid tumours can very closely resemble proximal-variant epithelioid sarcomas. Rhabdoid tumours display biallelic inactivation of *SMARCB1* as the main genetic aberration within an otherwise genomically silent background [17]. However, SMARCB1 losses have also been found to be secondary events in transitioning or compound tumours [18,19]. Here, we use next-generation sequencing to examine epithelioid sarcoma, to gain an overall understanding of its genomic landscape and the role of SMARCB1 loss in its pathogenesis.

Materials and methods

Samples

Ten samples underwent whole genome, exome, and/or transcriptome sequencing (Table 1). These comprised three cell lines and seven snap-frozen primary tumour samples, from the University of British Columbia/Vancouver General Hospital Sarcoma Tumor Bank, the Lunenfeld-Tanenbaum Research Institute Tumor Bank, and the Cleveland Clinic. The tumour content of the frozen specimens ranged from 40% to 80% based on H&E evaluations and APOLLOH tumour content predictions of the sequenced DNA (Table 1). All patient samples were obtained with consent and procedures approved by institutional review boards. The University of British Columbia ethics approval code was H08 01411.

Cell lines

Cell lines Epi544 [20] and HS-ES [21,22] were obtained from the original developing laboratories, and VAESBJ, G401, and 293 t cells were purchased from the American Type Culture Collection (Manassas, VA, USA). All lines were grown in DMEM supplemented with 10% fetal bovine serum.

Extractions, sequencing, and analysis

Frozen sections were used to check for tumour content via H&E and for *SMARCB1* negativity by immunohistochemistry. The frozen samples were homogenized in liquid nitrogen with a mortar and pestle. Nucleic acids were then extracted using QIAamp DNA and Qiagen RNeasy minikits (Qiagen, Alameda, CA, USA). The quality of RNA samples was checked on an Agilent 2100 bioanalyzer (Agilent, Santa Clara, CA, USA) and samples with RNA integrity number greater than 8 were considered for sequencing. Similarly, DNA samples were run on 1% ethidium bromide agarose gels to confirm lack of degradation. For cell lines, homogenization was performed using Qiashredder columns. The nucleic acids were submitted to Canada's Michael Smith Genome Sciences Centre for sequencing using Illumina HiSeq platforms. All DNA samples were also applied to Affymetrix SNP6.0 arrays for copy number analysis. Bioinformatic analyses were performed as described previously [23]. Copy number analysis was done using APOLLOH [24] and HMMCopy [25], which predict and correct for normal contamination; fusion analysis was done with DeFuse [26] and single nucleotide variants were called using SNVMix [27] and mutationSeq [24]. For matched cases, mutation calls in common between the tumour and normal pairs were eliminated to focus on somatic changes. Mutation rate analysis and collection of comparison data were carried out using MuTect and as reported previously [28]. Cell line expression comparison was made using the methods described previously and combining our data with prior cell line RNA-seq expression data.

Immunohistochemistry

Immunohistochemistry was performed using a semi-automated Ventana Discovery XT (Ventana Medical Systems, Tucson, AZ, USA) with 4-μm frozen or paraffin block sections. Primary antibodies were used in variable dilutions with a 2-h incubation followed by a 16-min incubation with pre-diluted HRP-conjugated anti-mouse secondary antibody. Images were obtained using the ScanScopeXT digital scanning system (Aperio Technologies, Vista, CA, USA). The antibodies used were SMARCB1 (BD Biosciences, San José, CA, USA; 612110), SMARCA2 (Sigma-Aldrich, St Louis, MO, USA; HPA029981), SMARCA4 (Abcam, Cambridge, MA, USA; ab110641), CDKN2A (Ventana, Tucson, AZ, USA; 725–4713), and ARID1A (HPA005456).

Fluorescent *in situ* hybridization (FISH)

FISH was performed on 4-μm sections of paraffin-embedded blocks of formalin-fixed cell line blocks and primary tissues. Two sets of probes were used. Set 1 included green fluorescent RP11-71G19 to detect *SMARCB1* and red fluorescent RP11-262A13 as a telomeric marker for chromosome 22. Set 2 used a break-apart protocol to detect translocations involving *SMARCB1*; it included green fluorescent RP11-80O7 and RP11-76E8 at the 3′ end and red fluorescent CTD-2376E20 and RP11-61P17 at the 5′

Table 1. Overview of the discovery cohort. All cases lacked expression of SMARCB1 protein, confirmed by immunohistochemistry of the frozen specimen or based on the original pathology reports. The diagnosing pathologist determined the subtypes. The subtyping of cell lines was based on histology and location presented in the original publications [20–22,34]. The genomic methodologies applied to each case are indicated in Figure 3. 'Matched' refers to the availability of genomic data from normal tissue from the same individual. All the analyses for the matched cases were carried out with the subtraction of the germline variants thereby identified. Whole genome coverage was 60× for tumour and 30× for matched normal tissue. The indicated status of SMARCB1 is based on whole genome shotgun sequencing (WGSS) analysis when available and on SNP6.0 chip for cases without WGSS. For cell lines, MLPA was used to determine *SMARCB1* gene status.

Type	ID	Subtype	Tumour content	*SMARCB1* gene status
Unmatched tumour	T1	Classic	40% (Histology)	Fusion, neutral CN
Unmatched tumour	T2	Classic	N/A	Intact
Matched tumour	T3	Classic	40% (APOLLOH), 40% (Histology)	Het del
Matched tumour	T4	Classic	42% (APOLLOH), 50% (Histology)	Het del
Matched tumour	T5	Classic	70% (APOLLOH), 80% (Histology)	Hom del
Unmatched tumour	T6	Proximal	N/A	Hom del
Matched tumour	T7	Proximal	40% (APOLLOH), 66% (Histology)	Het del
Cell line	Epi544	Classic	100%	Hom del
Cell line	HSES	Proximal	100%	Het del
Cell line	VAESBJ	Proximal	100%	Hom del of exon 1

N/A = not available; CN = copy number; Het del = heterozygous deletion; Hom del = homozygous deletion.

end of the gene. The slides were baked overnight at 70 °C, deparaffinized in xylene, dehydrated with ethanol washes, incubated for 1 h in 10 mM citric acid at 80 °C, and treated with pepsin for 20 min at 37 °C. Probes were hybridized at 37 °C for 16 h. DAPI II was used to outline the nuclei.

Methylation-specific PCR (MSPCR)

Bisulphite conversion was done using Qiagen Epi-Tect Bisulfite kits (Qiagen). Methylation-specific PCR primers were designed using MSPPrimer [29] (http://www.mspprimer.org/) and three sets were optimized to cover the CpG island of *SMARCB1*. CpG methylated Jurkat genomic DNA (New England Biolabs, Ipswich, MA, USA) was used as a positive control.

Quantitative PCR

RNeasy mini kits (Qiagen) were used for RNA extraction from cell lines, subsequently converted to cDNA by a high-capacity cDNA reverse transcription kit (Applied Biosystems, Foster City, CA, USA). Taqman expression assays were performed on an ABI 7500 fast real-time PCR system and normalization was done to *TBP*, *ACTB* or *U6* levels.

Multiplex ligation-dependent probe amplification (MLPA)

Pre-designed MLPA probe sets for *SMARCB1* (MRC-Holland, Amsterdam, The Netherlands) were used and post-ligation amplified targets were analysed on a 3130xl Genetic Analyzer (Applied Biosystems).

MicroRNA assays and expression

To evaluate microRNA levels, Taqman assay probes (Cat# 4427975) miR-206 (000510), miR-193a-5p (002281), and miR-671-5p (197646-mat) were used. Human lentiviral miRNA inhibitor vectors (GeneCopoeia, Rockvilee, MD, USA) with mCherry tags on an AM03 backbone were co-transfected with lentiviral packaging vectors pCMV-VSVG and pCMV-dR8.91 into HEK293T cells. The generated viral particles were collected and applied to HSES. Transduced cells were selected with hygromycin at 500 µg/ml for 1 week.

siRNA and growth curve analysis

siRNAs against *SMARCA4* were obtained from Life Technologies SureSelect collection (siRNA#1:s13141, siRNA#2:s13139). Various amounts of siRNA (10–50 nM) and 3–9 µl of RNAiMax Lipofectamine (Life Technologies, Grand Island, NY, USA) were incubated with the target cells in six-well plates. Optimal knockdown was assessed via western blot analysis 72 h after siRNA addition. Greatest knockdown without major cell death was achieved with 50 nM siRNA and 8 µl of RNAiMax Lipofectamine. Transfections were carried out in reverse with trypsinized and counted cells (200 000 cells per well of six-well plates). For growth curve analysis, 48 h after the siRNA transfection, cells were reseeded into 96-well plates at 500 cells per well, with four replicates per transfection. The plates were incubated in an IncuCyte ZOOM® 37 °C and 5% CO_2 incubator for a week. Four images per well were collected and confluence was determined using the ZOOM® software using phase-contrast only conditions.

Co-immunoprecipitation and western blotting

Nuclear extracts for immunoprecipitation were prepared using the NE-PER nuclear and cytoplasmic extraction kit (Thermo Scientific: 78833). For each sample, 250 µl at 2.0 mg/ml was prepared and incubated overnight with 2 µg of either SMARCC1 (Santa Cruz Biotechnology, Santa Cruz, CA, USA: 9746) or goat IgG (Santa Cruz Biotechnology: 2028) antibodies at 4 °C. The following day, protein G Dynabeads (Life Technologies: 10004D) were added and incubated at 4 °C for 3 h. Beads were

then washed three times with RIPA buffer and resuspended in reducing SDS gel-loading buffer. SDS-PAGE was carried out in 7–12% polyacrylamide gels. After transfer, each nitrocellulose membrane was incubated with primary antibodies in 5% w/v skimmed milk for 2 h, washed with PBST, followed by incubation with HRP- or fluorescent-tagged secondary antibody (1:10 000) for 1 h. The membranes were visualized under a LI-COR Odyssey CLx (LI-COR, Lincoln, NE, USA) or with a G:Box Chemi XRQ (Syngene, Cambridge, UK) after addition of Supersignal Western Femto substrate (Thermo Scientific, Waltham, MA, USA). The primary antibodies used were SMARCC1 (Santa Cruz Biotechnology: 9746; 1:1000); ARID1A (Bethyl Laboratories, Montgomery, TX, USA: A301-041A; 1:1000); PBRM1 (Santa Cruz Biotechnology: 390095; 1:500); SMARCA4 (Santa Cruz Biotechnology: 17796; 1:500); SMARCC2 (Bethyl Laboratories: A301-039A; 1:3000); SMARCD1 (Bethyl Laboratories: A301-595A; 1:3000); SMARCE1/BAF57 (Bethyl Laboratories: A300-810A; 1:3000); ACTL6A/BAF53A (Bethyl Laboratories: A301-391A; 1:3000); SMARCB1 (BD Biosciences: 612111; 1:500), and VIN/Vinculin (Santa Cruz Biotechnology: 5573; 1:1000).

Results

Epithelioid sarcoma has a complex genome

An overview of the discovery cohort is shown in Table 1. Unlike rhabdoid tumours (which are SMARCB1-negative) [17], genomic analysis of epithelioid sarcoma reveals a complex karyotype. There is evidence of multiple copy number gains and losses throughout the genome (Figure 1). As expected, the normal blood sample used as a control displayed minimal copy number changes. Additionally, samples of small cell carcinoma of the ovary, hypercalcaemic type (SCCOHT), thought to belong to the rhabdoid tumour family [30], showed far fewer copy number changes than epithelioid sarcoma. The most prominent regions of copy number loss were in 22q11 and 12p13. A comprehensive list of the copy number changes per gene can be found in Supplementary Table 1.

Similarly, an abundance of translocations was observed (Supplementary Figure 2A). Samples had between 21 and 124 non-read-through gene fusions. Of these, only one to six open reading frame fusions per sample existed. Open reading frame fusions are predicted to be transcribed with the fusion partners maintaining their normal reading frame, and thus would be ideal to look for gain-of-function translocations. There were no recurrent open reading frame fusions of coding genes that were not a result of predicted read-through or alternative splicing events. Noteworthy was a fusion involving *SMARCB1* and *WASF2* in sample T1, which had a normal *SMARCB1* copy number from SNP6.0 data. Fluorescent *in situ* hybridization (FISH) on sample T1 using break-apart probes confirmed 3' end loss of *SMARCB1* in two alleles; however, it also revealed two intact alleles in the majority of tumour cells (Supplementary Figure 2B). This fusion would lead to the elimination of the SNF5 homology domain from the affected allele and would thus be detrimental to the normal interactions of SMARCB1.

In addition to the structural complexity observed, whole genome sequencing of epithelioid sarcoma revealed a high mutational burden. Figure 2 shows a comparison of the point mutation rate of the four matched epithelioid sarcoma cases with published data from The Cancer Genome Atlas (TCGA) [28]. Whereas the SMARCB1-negative paediatric rhabdoid tumours are at the extreme low end, epithelioid sarcoma has an intermediate mutational burden comparable to that of ovarian cancers and glioblastoma multiforme. Overall, there was an abundance of C-to-T transitions (Supplementary Figure 7). However, we did not find strong evidence for gain of copy or overexpression of APOBEC family or AICDA enzymes, which are known to cause cytidine deamination.

SMARCB1 is the most frequently mutated gene

To identify significant mutations, we focused on somatic calls within the four matched whole genome sequencing (WGSS) data. The exome, whole transcriptome sequencing (WTSS), and SNP6.0 data were then used to supplement any mutations seen in the WGSS analysis. The results are summarized in Figure 3. The most significant gene was *SMARCB1*. Several genes in 22q11 and 12p13 also showed copy number loss. Although several areas with gains of copy number were observed, there were no recurrent high-level amplifications (defined as ≥ 5 copies). *CDKN2A* is a well-established cell cycle regulator that was found to have deletions in two tumour cases and two cell lines.

SMARCB1 inactivation

Despite the high rate of mutations affecting *SMARCB1*, we did not find biallelic inactivation in every case. We therefore set out to examine this further in cell lines. FISH against *SMARCB1* confirmed the SNP6.0 findings (Figures 4A and 4B): Epi544 had homozygous deletion of the gene, while VAESBJ had maintained two copies and HSES had maintained one allele. However, because of the low resolution of the SNP6.0 and FISH results, we further used PCR across exons (Figure 4B) and multiplex ligation-dependent probe amplification (MLPA) (Supplementary Figure 3A) to evaluate the copy number changes in these cell lines. As reported previously [31], VAESBJ had homozygous deletions in the promoter and exon 1; however, HSES had maintained a seemingly intact allele. Sanger sequencing across the gene in HSES failed to identify any point mutations, in agreement with the exome and WTSS results. Therefore, this cell line seems to be an appropriate model for the evaluation of a possible epigenetic second hit to SMARCB1 in

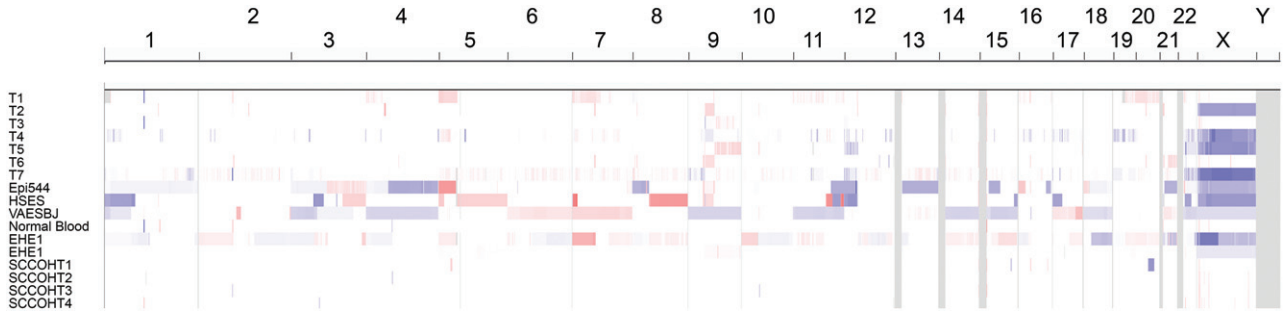

Figure 1. Virtual karyotype of epithelioid sarcoma. Blue indicates loss of copy and red, copy number gain. Chromosome numbers are indicated on the top panel. The green bar to the right highlights the epithelioid sarcoma cases, which show frequent aberrations in copy number. Below these, highlighted by the brown side bar, other tumours analysed in parallel with the epithelioid sarcomas are displayed for comparison. These include epithelioid haemangioendothelioma (EHE), which is in the differential diagnosis of epithelioid sarcoma, and small cell carcinoma of the ovary, hypercalcaemic type (SCCOHT), considered by some to belong to the rhabdoid tumour family [30]. Of note is sample T7, with an abundance of small copy number changes, which was the only sample with prior chemotherapy/radiation therapy.

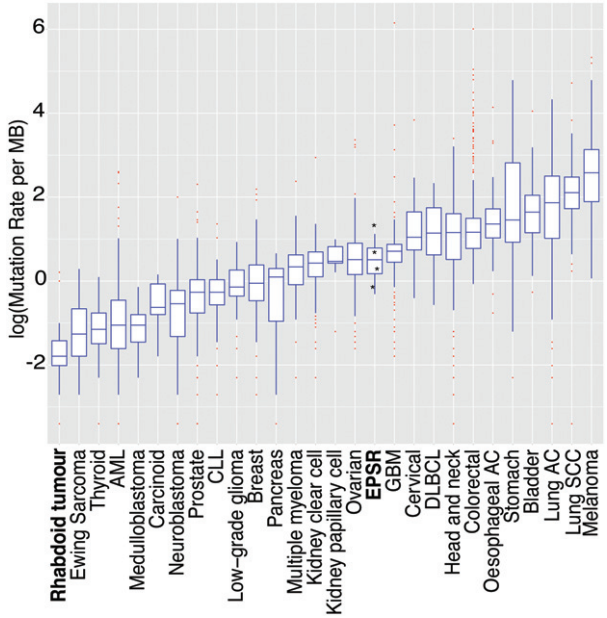

Figure 2. Coding somatic point mutation rate in epithelioid sarcoma compared with other tumours. Data from all tumours other than epithelioid sarcoma are from The Cancer Genome Atlas (TCGA) [28]. AML = acute myeloid leukaemia; CLL = chronic lymphocytic leukaemia; CCRCC = clear cell renal cell carcinoma of kidney; PRCC = papillary cell carcinoma of kidney; EPSR = epithelioid sarcoma; GBM = glioblastoma multiforme; DLBCL = diffuse large B-cell lymphoma; head and neck = head and neck squamous cell carcinoma; oesophageal AC = oesophageal adenocarcinoma; LAC = lung adenocarcinoma; lung SCC = lung squamous cell carcinoma. For data derived from genome sequencing, the mutation rate in the coding regions was calculated for comparison to those samples with exome sequencing.

at least some cases of epithelioid sarcoma. Because of very low (but non-zero) mRNA levels of *SMARCB1* in HSES, we focused on transcriptional silencing mechanisms. In agreement with previous literature [10], we did not find evidence of promoter methylation using methylation-specific PCR (Figure 4C). Additionally, long-term exposure to decitabine did not restore the expression of the remaining allele (Figure 4D).

We next looked at the levels of some of the miRNAs previously suggested to suppress *SMARCB1* [14,15] in epithelioid sarcoma. These microRNAs (discovered through their differential expression between epithelioid sarcomas and malignant rhabdoid tumours) include miR-193a-5p, miR-206, miR-381, and miR-671-5p. Some, in particular miR-206, were shown to down-regulate *SMARCB1* upon overexpression in fibroblast lines [14]; however, their evaluation in an epithelioid sarcoma model is lacking. Since we found HSES to be an example of an epithelioid sarcoma with a genetically intact but silenced *SMARCB1* allele, we decided to use this *in vitro* model to evaluate the aforementioned microRNAs. Neither miR-206 nor miR-193a-5p was uniquely up-regulated in HSES, although miR-193a-5p had prominent levels in epithelioid sarcoma lines (Figure 4E). Furthermore, competitive inhibition of miR-206 failed to increase *SMARCB1* transcripts, despite leading to up-regulation of three other known targets of miR-206 (Supplementary Figure 3B). We also did not find inhibition of miR-193a5p, miR-381, or miR-671-5p to increase *SMARCB1* transcripts significantly (data not shown).

CDKN2A loss in epithelioid sarcoma

CDKN2A has been shown to be critical for the action of SMARCB1 as a tumour suppressor in rhabdoid tumours [32]. It was somewhat surprising to find cases with the homozygous deletion of both *SMARCB1* and *CDKN2A*. We therefore used an epithelioid sarcoma tissue microarray [20] to evaluate CDKN2A expression in tumour samples. We limited our observation to cores with evidence of strong positive staining for epithelioid sarcoma biomarkers in at least two additional immunohistochemistry stains, to ensure good quality of the cores (Supplementary Table 2). Furthermore, when multiple cores were available per case, we only considered cases with concordant results. Out of 16 cases, six (37%) showed loss of CDKN2A in more than 90% of cells (Supplementary Table 2). Interestingly, two cases showed very strong staining for CDKN2A. This suggests that in epithelioid sarcoma, SMARCB1 loss does not dictate

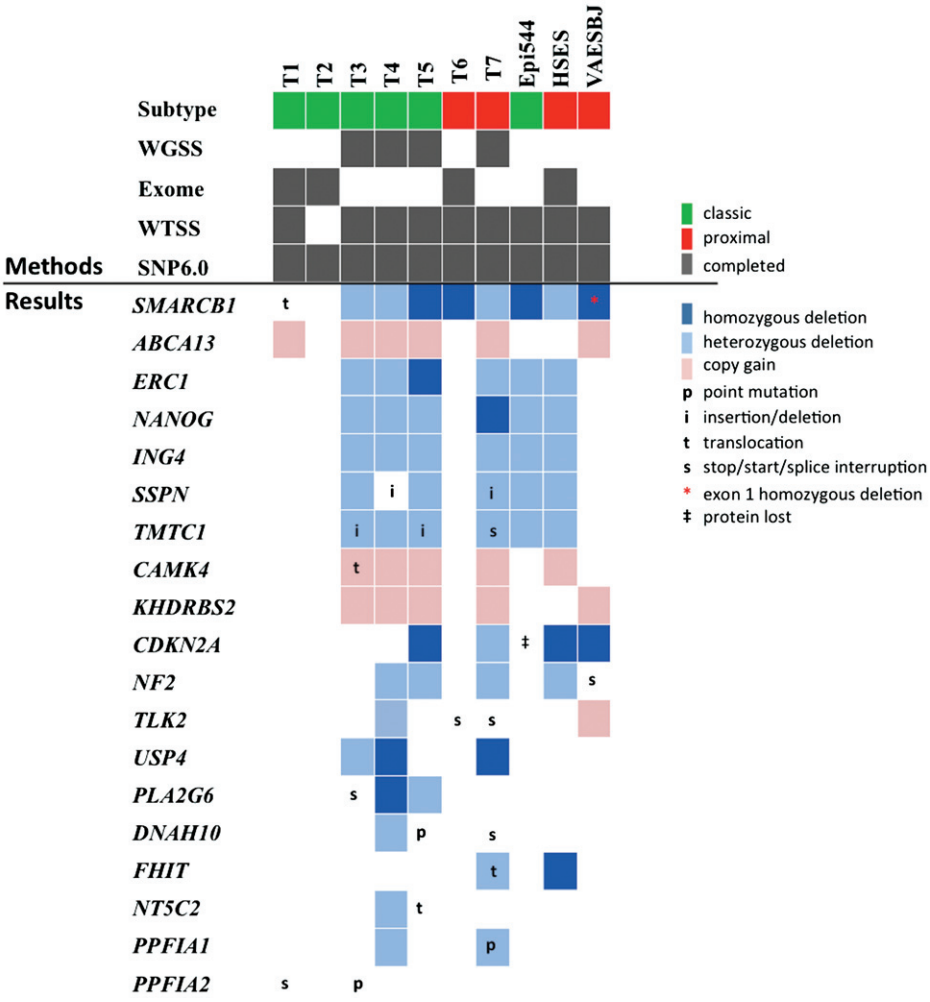

Figure 3. Summary of recurrent mutations. For samples T3, T4, T5, and T7, matched normal tissue was sequenced, and the somatic calls in these samples were used to identify candidate genes. Genes are ranked based on the frequency of mutations and then on the speculated impact of the change. For instance, homozygous deletions would be considered more deleterious than heterozygous deletions or slight gains of copy number. Regions of 22q11 and 12p13 had multiple genes with heterozygous deletions in several cases and representative genes are shown. Supplementary Table 1 includes the complete lists of genes affected in these regions. For copy number, because of higher resolution, MLPA and WGSS took priority over SNP6.0 when multiple methods were available.

the expression of CDKN2A, and thus *CDKN2A* mutations as seen in our cohort may provide additional proliferative advantages to the tumour cells. In addition to T5 and T7, all epithelioid sarcoma cell lines had also lost *CDKN2A* transcription (Supplementary Table 1).

Cell line expression profiling

Using recently published comprehensive expression data [33], we combined our RNA-seq data from the epithelioid sarcoma cell lines with that of 675 other human cancer cell lines, looking for clustering with tumours of a particular tissue type (Figure 5). There were large clusters of breast, lymphoid, brain, pancreatic, lung, colorectal, kidney, ovarian, and skin cancer cell lines, as previously described. Certain source tissue types, such as lung and pancreas, had multiple clusters. Epithelioid sarcoma lines, especially Epi544 and HSES, clustered closely with one another. VAESBJ was more distant but this is not surprising given the unique and unusually aggressive original presentation of its primary tumour [34]. The epithelioid sarcoma lines did not form a clear cluster within any particular tissue type. Kidney tumour lines were the most abundant in clusters containing epithelioid sarcoma, followed by ovarian and pancreatic lines. Because of the lack of a clear differentiation pattern, and due to the critical role of SMARCB1 in the tumourigenesis of epithelioid sarcoma and in differentiation [35], we examined the expression levels of this and other key SWI/SNF members across cell lines (Figure 5). Most lines had maintained expression of the core SWI/SNF members and as expected, epithelioid sarcoma lines were among the few with reduced *SMARCB1* expression. The maintenance of high levels of expression of other SWI/SNF members in epithelioid sarcoma lines, as well as positive ARID1A and SMARCA2 protein staining in tissue samples (Supplementary Figure 4 and Supplementary Table 2), prompted us to explore the epithelioid sarcoma SWI/SNF complex further *in vitro*.

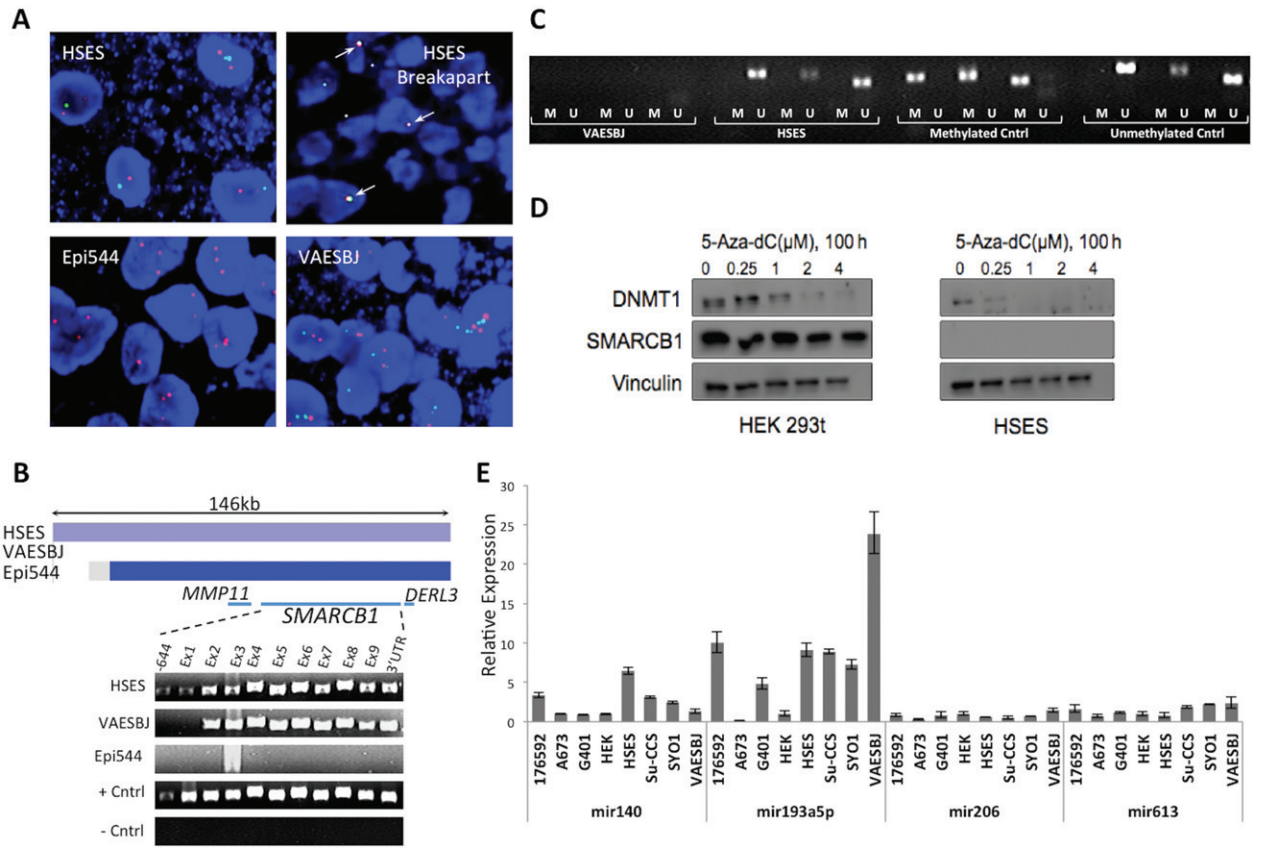

Figure 4. *SMARCB1* inactivation. (A) Fluorescent *in situ* hybridization (FISH) on cell lines. Apart from the upper right-hand panel, green signals represent *SMARCB1* and red, a marker in the telomeric region of chromosome 22. The top-right panel is a 'break-apart' FISH showing lack of translocation in HSES, with red and green probes at the centromeric and telomeric ends of *SMARCB1*, respectively. (B) PCR across all exons confirming the presence of a *SMARCB1* allele in HSES. SNP6.0 results are also demonstrated. The lower resolution of SNP6.0 did not identify the loss of exon 1 in VAESBJ. (C) Methylation-specific PCR at the promoter region of *SMARCB1*. (D) Long-term decitabine treatment does not restore SMARCB1 in HSES. DNMT1 down-regulation shows the efficacy of decitabine treatment. (E) MicroRNA levels across cell lines, normalized to U6 levels. miR-206 and miR-193a-5p have been previously suggested to cause *SMARCB1* loss in epithelioid sarcoma [14,15]. In addition to miR-206, miR-613 is another microRNA predicted to target *SMARCB1* by Target Scan (http://www.targetscan.org/). miR-140 was a randomly chosen microRNA for comparison purposes. In addition to the epithelioid sarcoma cell lines (VAESBJ, HSES), the cell lines shown for comparison are 176592, A673, HEK293t, Su-CCS, and SYO1, all of which have prominent *SMARCB1* transcripts (Supplementary Figure 3C), and G401, which has a homozygous *SMARCB1* deletion (Supplementary Figure 3A).

The residual SWI/SNF complex and synthetic lethality

SMARCB1 is one of the core members of the SWI/SNF remodelling complex. We examined whether the remaining members of the complex associated with one another despite loss of SMARCB1. We used SMARCC1 as bait to pull down the complex based on previous success with this approach [36]. Co-immunoprecipitation showed that in the VAESBJ and HSES cell lines (as in the SMARCB1-null malignant rhabdoid tumour line G401, as well as the SMARCB1 wild-type 293 t cell line), SWI/SNF members still interacted with one another (Figure 6). Furthermore, VAESBJ seemed to be dependent on this residual complex, since with the knockdown of its core enzymatic unit SMARCA4, the tumour cells had significantly reduced proliferation. A similar effect was observed in G401 but not in the SMARCB1 wild-type 293 t cells (Figure 6). VAESBJ was used in this model because of greater efficiency of knockdown, whereas with HSES, good knockdown could not be produced. We also examined the efficacy of a newly developed SMARCA4 bromodomain inhibitor, PFI-3 (Sigma-Aldrich); however, this compound was not effective in reducing VAESBJ or G401 cellular proliferation (Supplementary Figure 6).

Discussion

Epithelioid sarcoma is a relatively understudied tumour, challenging to investigate because of the rarity of specimens as well as the tumour's inherent nature. Cases typically present as small indolent masses, and due to the close association of tumour and normal cells, it is difficult to obtain specimens of high tumour content. However, improved therapeutic options are desperately needed. The primary tumour can appear indolent, but the metastatic rate is 50% [5] with a median post-metastatic survival of only 8 months [37]. Currently, commonly used chemotherapies include

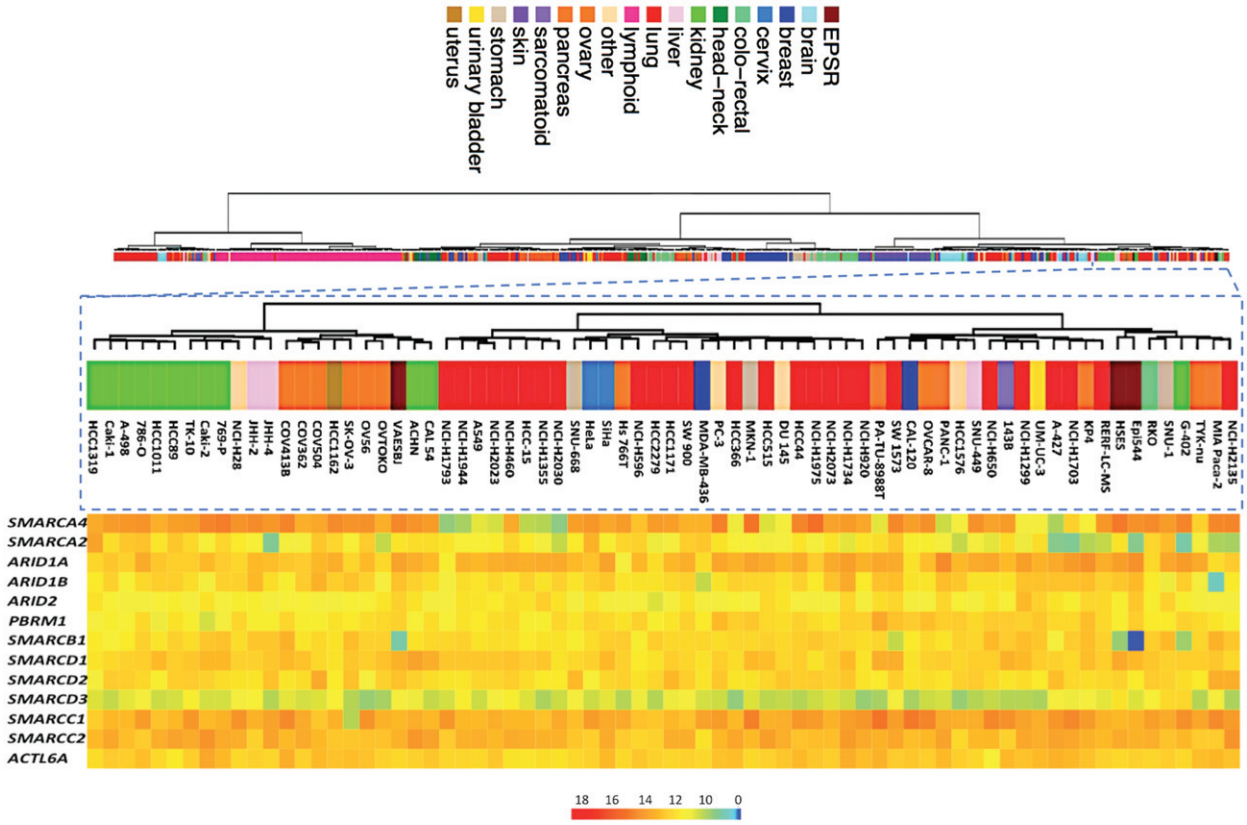

Figure 5. Cell line clustering. The top portion of the figure depicts the clustering of all lines, with the inset signifying the branch to which epithelioid sarcoma lines cluster. The mRNA levels of SWI/SNF genes are shown as a heat map in the bottom section.

ifosfamide and doxorubicin, but these are considerably less effective than in other soft tissue sarcomas [38]. There are recent reports of better success with gemcitabine/docetaxel [39] but there is much room for improvement. More recent studies have pointed out the hyperactivity of EGFR, MTOR, and C-MET pathways and have suggested combined inhibition of these pathways as experimental therapeutic options [40,41].

In the hopes of identifying additional therapeutic targets in epithelioid sarcoma, we investigated its genomic landscape using multiple techniques. Epithelioid sarcoma was revealed to have a complex genome with a high mutational burden; nevertheless, mutations in *SMARCB1* remained the most frequently recurring event. The genomic complexity and high mutation rate of epithelioid sarcoma contrast with rhabdoid tumour, a paediatric neoplasm also primarily driven by the loss of *SMARCB1* [17]. SWI/SNF has a role in double-stranded DNA repair [42,43], so aberrations in SWI/SNF resulting from SMARCB1 loss could potentially lead to the abundance of translocations observed in epithelioid sarcoma. We also noted the co-existence of CDKN2A and SMARCB1 loss in some tumours, which is counterintuitive given one of the known mechanisms through which SMARCB1 controls the cell cycle in rhabdoid tumour cells [32]. However, even in the *CDKN2A* mutant VAESBJ cell line, re-expression of SMARCB1 leads to growth arrest [31], and thus tumour formation via SMARCB1 loss in epithelioid sarcoma might be CDKN2A-independent. Despite the common loss of *SMARCB1* in rhabdoid tumours and epithelioid sarcoma, there are fundamental differences in clinical behaviour, genomics, and presumably mechanisms of oncogenesis separating these tumour types.

Furthermore, alleles with apparently intact *SMARCB1* coding sequences are present in some epithelioid sarcomas. The mechanism of SMARCB1 loss in such cases is yet to be elucidated; however, HSES appears to be a good *in vitro* model for further exploration of the mechanism of this 'second hit'. We did not find the microRNAs implicated in the literature to be involved in the silencing of *SMARCB1* in HSES.

The expression profile of epithelioid sarcoma cell lines does not correspond to a specific tissue type and its cell of origin remains unknown. However, we have identified the other cell lines that are most similar in expression pattern to the epithelioid sarcoma lines and noticed that these do not necessarily have expressional abnormalities in *SMARCB1* or other SWI/SNF genes. Furthermore, the residual SWI/SNF complex, upon which epithelioid sarcoma appears dependent for proliferation *in vitro*, opens up new therapeutic options. The core enzymatic unit of SWI/SNF, SMARCA4, is a particularly attractive target for molecular inhibition because it possesses ATPase as well as bromodomains. The bromodomain inhibitor PFI-3 was not particularly effective at suppressing the growth of epithelioid

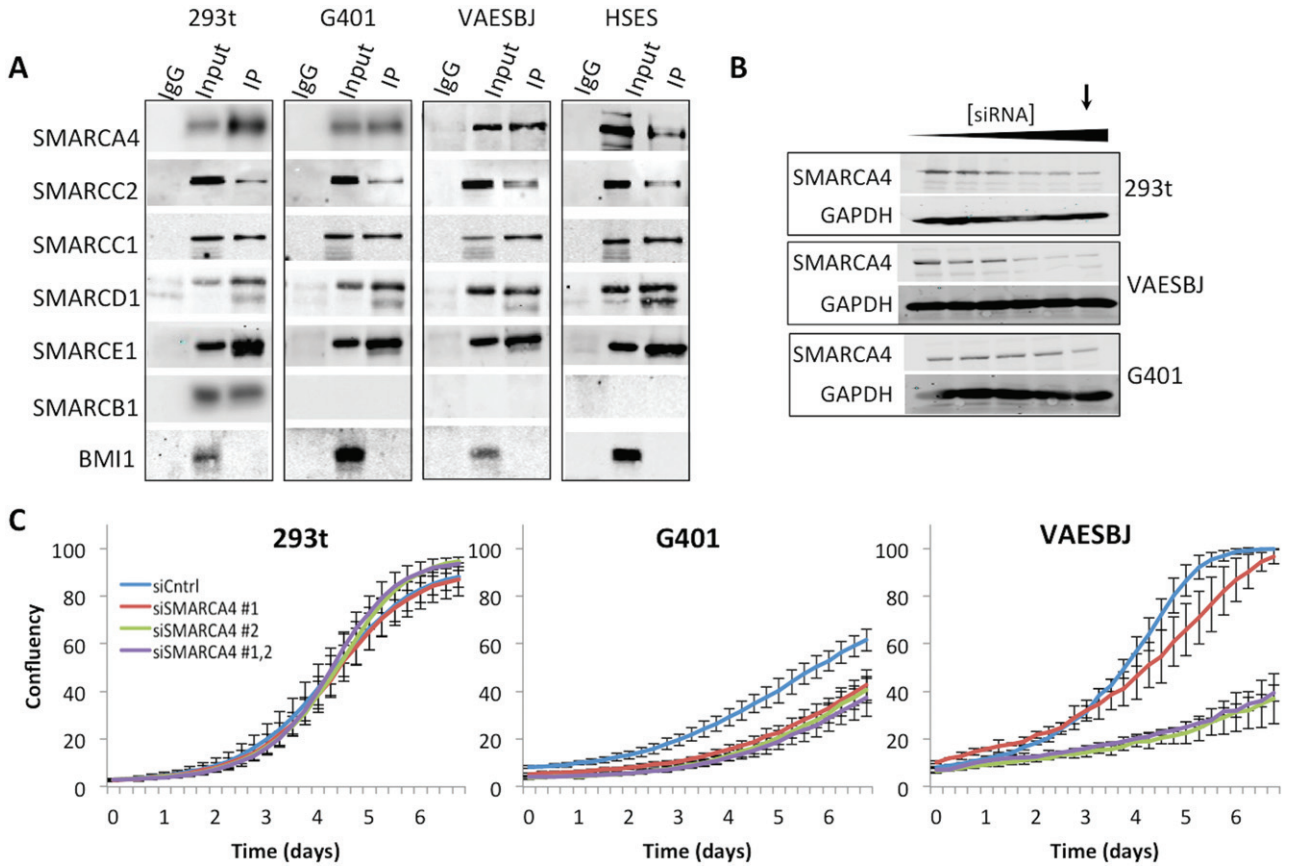

Figure 6. The residual SWI/SNF complex. (A) Co-immunoprecipitation of the SWI/SNF complex members via pull-down of SMARCC1. Despite the loss of SMARCB1 in the epithelioid sarcoma cell lines VAESBJ and HSES and the malignant rhabdoid tumour line G401, members of the SWI/SNF complex associate with one another. BMI1 is used as an input control and does not associate with SWI/SNF. (B) Western blots 3 days after RNAi transfection with siSMARCA4 #2. 10–50 nM siRNA was used, with doses increasing from left to right. The greatest knockdown condition (arrow, 50 nM siRNA) was used for evaluating effects on proliferation. (C) Impact of SMARCA4 loss on cellular proliferation in SWI/SNF wild-type 293 t and SMARCB1-deficient G401 and VAESBJ lines. The error bars are ± standard deviations. The siRNA knockdown achieves long-term effects, as shown by qPCR in Supplementary Figure 5.

sarcoma cells. We also noticed a tendency for increased proliferation of SWI/SNF wild-type 293 t cells on SMARCA4 knockdown, an observation that concords with the previously described tumour suppressor role of SMARCA4 [44]. Thus, although SMARCA4 inhibition might reduce tumour cell proliferation, there might be unexpected side effects on normal cells.

Acknowledgments

We would like to thank Dr Brian Rubin for providing two of the specimens used in this study. We are grateful to Dr Charles W Roberts and his group, who provided gracious guidance in their experimental approaches with the SWI/SNF complex. Christine Chow and Dongxia Gao at the Genetic Pathology Evaluation Centre performed and scored the IHC. We thank Dr Robin Jones for his support. TON is supported by the Canadian Cancer Society Research Institute (grant No 701582). FJ is supported by the Vancouver Coastal Health/Canadian Institute of Health Research MD/PhD studentship award. FJ, TON, and DGH are supported by The Terry Fox Research Institute New Frontiers in Cancer. This work was supported in part by grants to ILA and JSW from the Ontario Research Fund, and the Canadian Foundation for Innovation.

Author contribution statement

FJ wrote the manuscript. ILA and TON revised and edited the manuscript. FJ, AB, SS, TON, and DGH contributed to study design. FJ carried out the experiments and collected data. AB and KS did the bioinformatics analysis. BD and TON had evaluated the pathology of the samples used. NG, BD, JSW, and ILA contributed samples and nucleic acids to the discovery cohort. AL contributed to the TMA study.

References

1. Berger L. Synovial sarcomas in serous bursae and tendon sheaths. *Am J Cancer* 1938; **34:** 501–538.
2. Black WC. Synovioma of the hand. Report of a case. *Am J Cancer* 1936; **28:** 481–484.
3. Laskowski J. Sarcoma aponeuroticum. *Nowotwory* 1961; **11:** 61–67.

4. Enzinger FM. Epithelioid sarcoma. A sarcoma simulating a granuloma or a carcinoma. *Cancer* 1970; **26:** 1029–1041.
5. Sobanko JF, Meijer L, Nigra TP. Epithelioid sarcoma: a review and update. *J Clin Aesthet Dermatol* 2009; **2:** 49–54.
6. Guillou L, Wadden C, Coindre JM, et al. 'Proximal-type' epithelioid sarcoma, a distinctive aggressive neoplasm showing rhabdoid features. Clinicopathologic, immunohistochemical, and ultrastructural study of a series. *Am J Surg Pathol* 1997; **21:** 130–146.
7. Modena P, Lualdi E, Facchinetti F, et al. *SMARCB1/INI1* tumor suppressor gene is frequently inactivated in epithelioid sarcomas. *Cancer Res* 2005; **65:** 4012–4019.
8. Hornick JL, Dal Cin P, Fletcher CD. Loss of INI1 expression is characteristic of both conventional and proximal-type epithelioid sarcoma. *Am J Surg Pathol* 2009; **33:** 542–550.
9. Kohashi K, Izumi T, Oda Y, et al. Infrequent *SMARCB1/INI1* gene alteration in epithelioid sarcoma: a useful tool in distinguishing epithelioid sarcoma from malignant rhabdoid tumor. *Hum Pathol* 2009; **40:** 349–355.
10. Papp G, Changchien YC, Peterfia B, et al. SMARCB1 protein and mRNA loss is not caused by promoter and histone hypermethylation in epithelioid sarcoma. *Mod Pathol* 2013; **26:** 393–403.
11. Flucke U, Slootweg PJ, Mentzel T, et al. Re: Infrequent *SMARCB1/INI1* gene alteration in epithelioid sarcoma: a useful tool in distinguishing epithelioid sarcoma from malignant rhabdoid tumor: direct evidence of mutational inactivation of *SMARCB1/INI1* in epithelioid sarcoma. *Hum Pathol* 2009; **40:** 1361–1362; author reply 1362–1364.
12. Sullivan LM, Folpe AL, Pawel BR, et al. Epithelioid sarcoma is associated with a high percentage of *SMARCB1* deletions. *Mod Pathol* 2013; **26:** 385–392.
13. Le Loarer F, Zhang L, Fletcher CD, et al. Consistent *SMARCB1* homozygous deletions in epithelioid sarcoma and in a subset of myoepithelial carcinomas can be reliably detected by FISH in archival material. *Genes Chromosomes Cancer* 2014; **53:** 475–486.
14. Papp G, Krausz T, Stricker TP, et al. *SMARCB1* expression in epithelioid sarcoma is regulated by miR-206, miR-381, and miR-671-5p on both mRNA and protein levels. *Genes Chromosomes Cancer* 2014; **53:** 168–176.
15. Kohashi K, Yamamoto H, Kumagai R, et al. Differential microRNA expression profiles between malignant rhabdoid tumor and epithelioid sarcoma: miR193a-5p is suggested to downregulate *SMARCB1* mRNA expression. *Mod Pathol* 2014; **27:** 832–839.
16. Agaimy A. The expanding family of SMARCB1 (INI1)-deficient neoplasia: implications of phenotypic, biological, and molecular heterogeneity. *Adv Anat Pathol* 2014; **21:** 394–410.
17. Lee RS, Stewart C, Carter SL, et al. A remarkably simple genome underlies highly malignant pediatric rhabdoid cancers. *J Clin Invest* 2012; **122:** 2983–2988.
18. Donner LR, Wainwright LM, Zhang F, et al. Mutation of the *INI1* gene in composite rhabdoid tumor of the endometrium. *Hum Pathol* 2007; **38:** 935–939.
19. Kleinschmidt-DeMasters BK, Birks DK, Aisner DL, et al. Atypical teratoid/rhabdoid tumor arising in a ganglioglioma: genetic characterization. *Am J Surg Pathol* 2011; **35:** 1894–1901.
20. Sakharpe A, Lahat G, Gulamhusein T, et al. Epithelioid sarcoma and unclassified sarcoma with epithelioid features: clinicopathological variables, molecular markers, and a new experimental model. *Oncologist* 2011; **16:** 512–522.
21. Sonobe H, Ohtsuki Y, Sugimoto T, et al. Involvement of 8q, 22q, and monosomy 21 in an epithelioid sarcoma. *Cancer Genet Cytogenet* 1997; **96:** 178–180.
22. Izumi T, Oda Y, Hasegawa T, et al. Prognostic significance of dysadherin expression in epithelioid sarcoma and its diagnostic utility in distinguishing epithelioid sarcoma from malignant rhabdoid tumor. *Mod Pathol* 2006; **19:** 820–831.
23. Shah SP, Kobel M, Senz J, et al. Mutation of *FOXL2* in granulosa-cell tumors of the ovary. *N Engl J Med* 2009; **360:** 2719–2729.
24. Ha G, Roth A, Lai D, et al. Integrative analysis of genome-wide loss of heterozygosity and monoallelic expression at nucleotide resolution reveals disrupted pathways in triple-negative breast cancer. *Genome Res* 2012; **22:** 1995–2007.
25. Ha G, Shah S. Distinguishing somatic and germline copy number events in cancer patient DNA hybridized to whole-genome SNP genotyping arrays. *Methods Mol Biol* 2013; **973:** 355–372.
26. McPherson A, Hormozdiari F, Zayed A, et al. deFuse: an algorithm for gene fusion discovery in tumor RNA-Seq data. *PLoS Comput Biol* 2011; **7:** e1001138.
27. Roth A, Ding J, Morin R, et al. JointSNVMix: a probabilistic model for accurate detection of somatic mutations in normal/tumour paired next-generation sequencing data. *Bioinformatics* 2012; **28:** 907–913.
28. Lawrence MS, Stojanov P, Polak P, et al. Mutational heterogeneity in cancer and the search for new cancer-associated genes. *Nature* 2013; **499:** 214–218.
29. Brandes JC, Carraway H, Herman JG. Optimal primer design using the novel primer design program: MSPprimer provides accurate methylation analysis of the ATM promoter. *Oncogene* 2007; **26:** 6229–6237.
30. Foulkes WD, Clarke BA, Hasselblatt M, et al. No small surprise – small cell carcinoma of the ovary, hypercalcaemic type, is a malignant rhabdoid tumour. *J Pathol* 2014; **233:** 209–214.
31. Brenca M, Rossi S, Lorenzetto E, et al. *SMARCB1/INI1* genetic inactivation is responsible for tumorigenic properties of epithelioid sarcoma cell line VAESBJ. *Mol Cancer Ther* 2013; **12:** 1060–1072.
32. Oruetxebarria I, Venturini F, Kekarainen T, et al. $p16^{INK4a}$ is required for hSNF5 chromatin remodeler-induced cellular senescence in malignant rhabdoid tumor cells. *J Biol Chem* 2004; **279:** 3807–3816.
33. Klijn C, Durinck S, Stawiski EW, et al. A comprehensive transcriptional portrait of human cancer cell lines. *Nature Biotechnol* 2015; **33:** 306–312.
34. Helson C, Melamed M, Braverman S, et al. VA-ES-BJ – an epithelioid sarcoma cell-line. *Int J Oncol* 1995; **7:** 51–56.
35. You JS, De Carvalho DD, Dai C, et al. SNF5 is an essential executor of epigenetic regulation during differentiation. *PLoS Genet* 2013; **9:** e1003459.
36. Helming KC, Wang X, Wilson BG, et al. ARID1B is a specific vulnerability in *ARID1A*-mutant cancers. *Nature Med* 2014; **20:** 251–254.
37. de Visscher SA, van Ginkel RJ, Wobbes T, et al. Epithelioid sarcoma: still an only surgically curable disease. *Cancer* 2006; **107:** 606–612.
38. Wolf PS, Flum DR, Tanas MR, et al. Epithelioid sarcoma: the University of Washington experience. *Am J Surg* 2008; **196:** 407–412.
39. Pink D, Richter S, Gerdes S, et al. Gemcitabine and docetaxel for epithelioid sarcoma: results from a retrospective, multi-institutional analysis. *Oncology* 2014; **87:** 95–103.
40. Imura Y, Yasui H, Outani H, et al. Combined targeting of mTOR and c-MET signaling pathways for effective management of epithelioid sarcoma. *Mol Cancer* 2014; **13:** 185.
41. Xie X, Ghadimi MP, Young ED, et al. Combining EGFR and mTOR blockade for the treatment of epithelioid sarcoma. *Clin Cancer Res* 2011; **17:** 5901–5912.
42. Park JH, Park EJ, Lee HS, et al. Mammalian SWI/SNF complexes facilitate DNA double-strand break repair by promoting γ-H2AX induction. *EMBO J* 2006; **25:** 3986–3997.
43. Chai B, Huang J, Cairns BR, et al. Distinct roles for the RSC and Swi/Snf ATP-dependent chromatin remodelers in DNA double-strand break repair. *Genes Dev* 2005; **19:** 1656–1661.
44. Jelinic P, Mueller JJ, Olvera N, et al. Recurrent *SMARCA4* mutations in small cell carcinoma of the ovary. *Nature Genet* 2014; **46:** 424–426.

SUPPORTING INFORMATION ON THE INTERNET

The following supporting information may be found in the online version of this article:

Figure S1. Histology of epithelioid sarcoma.

Figure S2. (A) Circos plots revealing a prominent occurrence of rearrangements in cases of classic (T1, T4, T5) and proximal (T7) epithelioid sarcomas as well as cell lines (Epi544). (B) An interesting open reading frame fusion of *SMARCB1* in T1, with the SNF5 homology domain interrupted.

Figure S3. (A) MLPA showing loss of all of SMARCB1 in Epi544 and G401, while VAESBJ has homozygous deletion of exon 1 (arrow). (B) Results of microRNA inhibition with anti-miR Sponge vectors in HSES. (C) Quantitative PCR of *SMARCB1* in cell lines evaluated for the microRNA levels in Figure 5E.

Figure S4. Representative immunohistochemistry results from TMA.

Figure S5. qPCR post SMARCA4 knockdown at 2 days and 1 week post-transfection.

Figure S6. PFI-3 is a bromodomain inhibitor of SMARCA4.

Figure S7. The somatic point mutational patterns in the whole genome cases of epithelioid sarcoma with predicted probability greater than 0.9.

Table S1. has several sheets including the mutation calls from sequencing as well as the expression FPKM values of epithelioid sarcoma lines versus several comparator lines.

Table S2. A summary of the immunohistochemistry scores for CDKN2A, ARID1A, and SMARCA2 in the epithelioid sarcoma tissue microarray.